Suppression of Quantum Decoherence in Nonlocal Resistance Measurement

H. Aikawa, K. Kobayashi, S. Katsumoto, and Y. Iye
Institute for Solid State Physics, University of Tokyo, Chiba, Japan

Abstract. We have measured resistance of Aharonov-Bohm rings and found that the electron coherence is better retained in the nonlocal four-terminal measurement than in the conventional one. This configuration-dependent decoherence is providing an interesting issue on the mechanism of quantum decoherence.

1. Introduction

Quantum coherence is one of the most important topics in fundamental physics, and decoherence of electrons in solids is also a serious obstacle for the devices based on quantum mechanics. In mesoscopic physics, this problem has often been investigated using Aharonov-Bohm (AB) interferometers. It is well known that probes of a sample play an essential role in coherent transport, that has been successfully described within the framework of the Landauer-Büttiker (LB) formalism [1]. Here we present evidence that the quantum coherence itself is affected by the probe selection.

2. Experiment

Our plan of experiment is as follows. Prepare an AB ring with four probes: two of those are used as the current source and drain, and the voltage difference between the other two is measured. Figures 1 (a) and (b) illustrate the two probe configurations used in the present study. In the "local" or conventional setup in Fig. 1 (a), electric current I_{14} is applied through the sample and voltage difference across the ring V_{23} is measured, giving the resistance $R_{14,23}$. The other setup shown in Fig. 1 (b) is referred to as "nonlocal" setup that yields the nonlocal resistance $R_{12,43}$. Such a kind of nonlocal resistance arises as a result of coherent transport.

The measured AB ring shown in Fig. 1 (c) was made from two-dimensional electron system (mobility $\mu = 90\ \mathrm{m}^2/\mathrm{Vs}$, and sheet carrier density $n = 3.8 \times 10^{15}\ \mathrm{m}^{-2}$) in the GaAs/AlGaAs heterostructure using electron beam lithography followed by wet chemical etching. The electron mean free path $\sim 8\ \mu$m is larger enough than the length of the arm of the ring $\sim 2\ \mu$m, so that our sample is in the quasi-ballistic regime. One of the Ti/Au gates deposited on the ring was used to modulate the AB phase, with the others being kept open in the present study. Two samples with the same geometry were measured between 30 mK and 4.2 K by using a dilution refrigerator and standard lock-in technique, yielding almost the same result. Typical driving current used was $I_{14} = 3$ nA for the local measurement and $I_{12} = 15$ nA for the nonlocal measurement, that was chosen in order not to cause any heating effects.

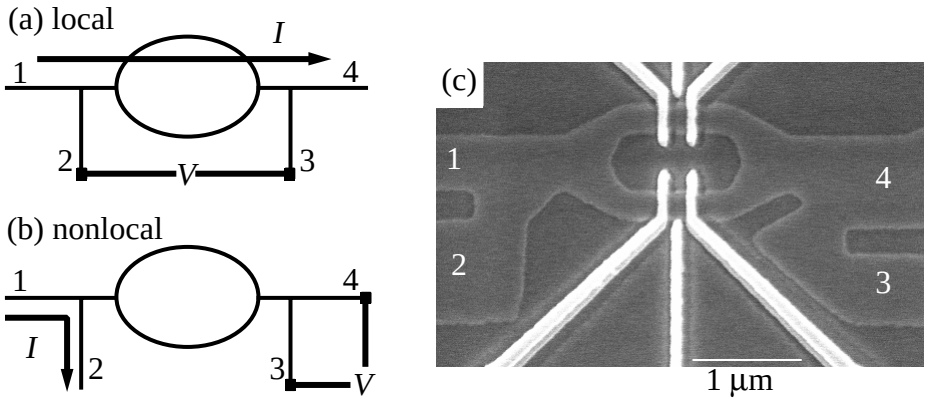

Figure 1. (a) "Local" setup ($I : 1 \rightarrow 4$, $V : 2 \rightarrow 3$) that gives conventional four-terminal resistance $R_{14,23}$. (b) "Nonlocal" setup ($I : 1 \rightarrow 2$, $V : 4 \rightarrow 3$) gives nonlocal resistance $R_{12,43}$. (c) Scanning electron micrograph of the AB ring. Only one of the six Ti/Au gates that were deposited on top of the arms of the AB ring was used, and the others were kept open during the experiment.

3. Results and Discussions

Figures 2 (a) and (b) show the typical AB oscillations for the local and the nonlocal setup, respectively. The same oscillation period 3.1 ± 0.5 mT was observed in both setups from the power spectrum as shown in Fig. 2 (c), which is in good agreement with the expected value from the sample geometry. However, two essentially different features were also seen.

One is the AB oscillation amplitude, which is about 20 % of the total signal on the average and 75 % at the largest in the nonlocal measurement, in contrast to at most a few percent in the local measurement as is usual in many previous AB experiments.

The other is the symmetry with respect to the magnetic field reversal. This can be readily seen from Fig. 3 where the AB oscillation components are plotted as gray-scale against the gate voltage. Almost symmetric magnetoresistance was observed in the local setup, while this is not the case in the nonlocal setup. This difference of the symmetry leads to the difference in the behaviour of the phase in the AB oscillation. In the local setup, the AB phase rigidity is maintained, while a continuous phase shift is realized in the nonlocal setup. The gate voltage (vertical axis) produces the AB phase modulation because it changes the electron density and hence the wave number of the traversing electrons underneath. When the electron density under the gate is assumed to decrease linearly with increasing negative gate voltage V, then the phase modulation $\Delta\theta$ is given as [2]

$$\Delta\theta = 2\pi \frac{d}{\lambda_{\rm F}} \left(1 - \sqrt{1 - \frac{V}{V_{\rm dep}}} \right), \tag{1}$$

where d is the width of the gate electrode, $\lambda_{\rm F}$ the Fermi wave length, and $V_{\rm dep}$ the voltage required to deplete the electrons underneath. The green curve in Fig. 3 (b) represents the equiphase line expected from Eq. (1).

Now we demonstrate that the above-mentioned features are well explained within the LB framework [1]. The LB formula gives four-terminal resistance as

$$R_{mn,kl} = \frac{h}{2e^2} \frac{T_{km}T_{ln} - T_{kn}T_{lm}}{D}, \tag{2}$$

where $T_{ij} (\geq 0)$ is the transmission coefficient from the terminal j to i, and the denominator D is a quantity including all of the T_{ij}'s. This formula, originally applied to perfect coherent

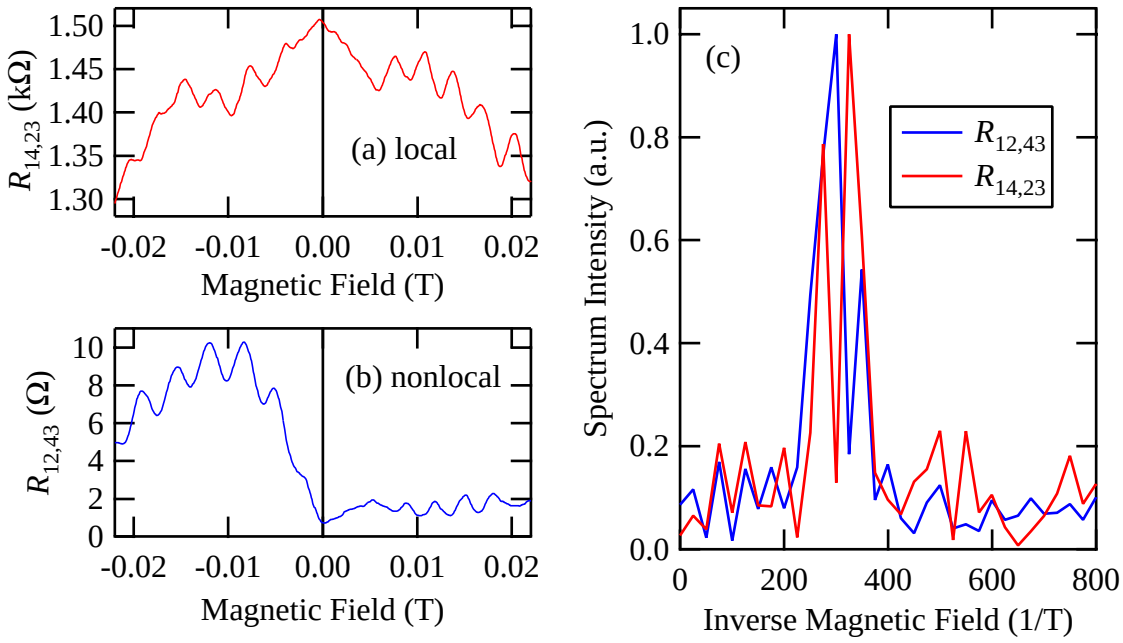

Figure 2. Typical AB oscillations taken at the base temperature (30 mK) for (a) the local and (b) the nonlocal setup. (c) Power spectrum of their oscillation component obtained by FFT after having subtracted a smooth background from the raw data.

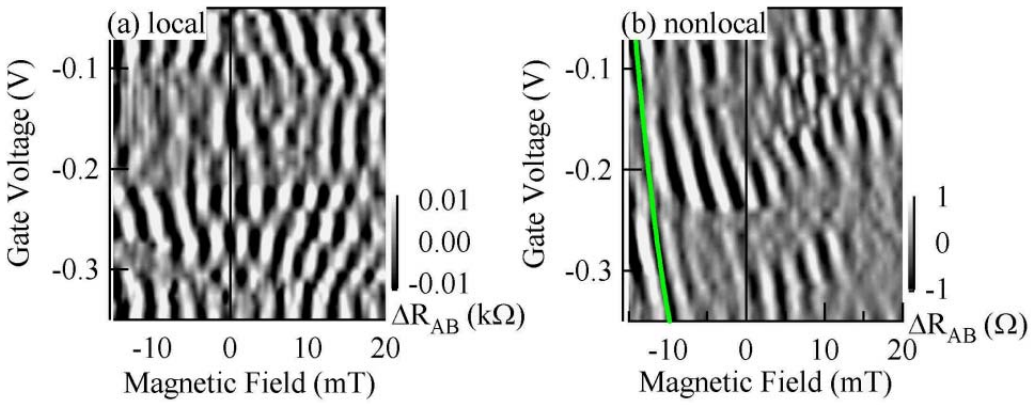

Figure 3. Gray-scale plots of the AB oscillation components as a function of a gate voltage which introduces the electrostatic modulation to the AB phase. (a) In the local setup, AB phase locking was observed (symmetric to the zero-field line) while (b) continuous change was seen in the nonlocal setup. The green curve in (b) represents the theoretically expected equiphase line (see text).

transpot, can be generalized to inlucde incoherent transport when we introduce an incoherent part into the transmission coefficients. Under this modification, the LB formula has the same functional form as the orignal one [4], thus the effect of decoherence is appropriately taken into account through the amplitude of the interference term in the transmission coefficients.

From our sample geometry, it is legitimate to approximate that $T_{12} = T_{21} = T_{34} = T_{43} \equiv T_0$, $T_{14} = T_{41} = T_{23} = T_{32} \equiv T_1$, $T_{13} = T_{31} = T_{24} = T_{42} \equiv T_2$, and $T_0 \gg T_1, T_2$. Then the LB formula gives the local and the nonlocal resistances as

$$R_{14,23} \sim \frac{h}{4e^2}\frac{1}{T_1 + T_2}, \tag{3}$$

$$R_{12,43} \sim \frac{h}{4e^2}\frac{T_1 - T_2}{T_0^2}, \tag{4}$$

respectively. Generally, T_1 and T_2 are expressed as $T_i = \alpha_i + \beta_i \cos(2\pi\phi/\phi_0 + \delta_i)$, where β_i represents the AB amplitude, α_i the other part of the transmission, ϕ the magnetic flux threading the ring, and $\phi_0 \equiv h/e$ the flux quantum. Although α_i also depends on the magnetic field and contains the terms due to the interference, $|\beta_i/\alpha_i|$ serves as a good measure of the coherence of traversing electrons.

The large AB oscillation amplitude in the nonlocal resistance is now understood from Eq. (4) because the non-oscillatory parts α_1 and α_2 cancels each other, which results in the large AB oscillation amplitude. In the local resistance, on the other hand, such an extraction of the oscillatory component cannot be realized. This qualitatively explains the observed difference of AB amplitude.

Another deduction from the LB formula is that under the simplification of the transmission coefficients mentioned above, the local resistance satisfies $R_{14,23}(B) \sim R_{14,23}(-B)$ like the two-terminal resistance, which leads to the locking of the AB phase. The nonlocal resistance, on the other hand, doesn't satisfy such a relation that the AB phase varies continuously with the gate voltage as seen in Fig. 3 (b).

So far, we have seen that the LB formula successfully describes the qualitative profiles of the results taken at the base temperature. Now we will focus on the temperature dependence of the AB oscillation. The data measured at various temperatures are presented in Figs 4 (a) and (b), from which a clear difference can be seen, i. e. the AB amplitude rapidly decreases with temperature in the local setup (Fig. 4 (a)), while it slowly degrades in the nonlocal case (Fig. 4 (b)). For quantitative comparison, we calculated the portion of the interference term δT_1 in the transmission coefficient through the ring T_1. Here, we presume that $T_1 \sim T_2$. Figure 4 (c) displays $\delta T_1/T_1$ as a function of the temperature, which can be fitted to $\exp(-aT)$ with a as a fitting parameter. We obtained $a = 0.70$ and $1.1\ \mathrm{K}^{-1}$ for the nonlocal setup, while $a = 2.3$ and $2.5\ \mathrm{K}^{-1}$ for the local setup.

Two factors are important for the reduction of the AB amplitude with temperature. One is the thermal broadening of the electron wave packets, which is expressed as $\beta_i \propto \exp(-\tau_L/\tau_{\mathrm{th}})$ in the ballistic regime, where $\tau_L = L/v_{\mathrm{F}}$ (L: the length of the arm of the ring, and v_{F}: the Fermi velocity) and $\tau_{\mathrm{th}} = \hbar/k_{\mathrm{B}}T$. The other is the quantum decoherence, which affects the coherence as $\beta_i \propto \exp(-\tau_L/\tau_\phi(T))$. When we take the thermal effect only into consideration, the coefficient a is expected to be $a \sim 1\ \mathrm{K}^{-1}$ for our sample, that is close to the observed value $a = 0.7 \sim 1.1\ \mathrm{K}^{-1}$ in the nonlocal setup. However, to account for the larger value in the local setup, quantum decoherence should be included in addition to the thermal effect.

Although the AB oscillations in both setups showed temperature dependence of the form $\exp(-aT)$, the problem is the difference in τ_ϕ between the two setups and how the quantum decoherence is suppressed in the nonlocal measurement. We speculate that the key difference lies in the decoherence caused by charge fluctuation induced by the transport current. It is suggested that the current causes charge fluctuations around the AB ring, yielding electron coherence time $\tau_\phi \propto T^{-1}$ [3], which is consistent with our result for the local setup. Such a mechanism, on the other hand, would be suppressed in the nonlocal measurement where no net current flows across the AB ring.

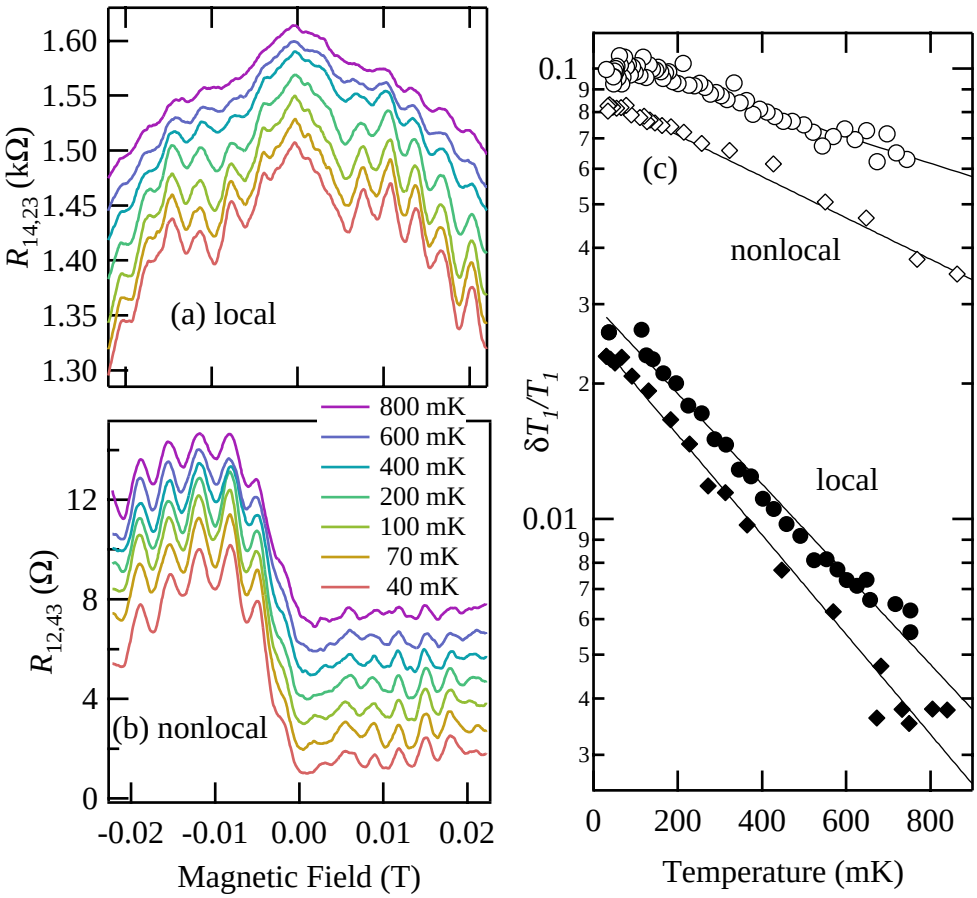

Figure 4. Raw data of AB oscillations taken at various temperatures for (a) the local setup and (b) the nonlocal setup. (c)Temperature dependence of the portion of the AB amplitude in the transmission coefficient $\delta T_1/T_1$ for the local (lower) and the nonlocal (upper) setup. The result for two different sample are displayed as circle and diamond. The solid lines are fits to the form $\exp(-aT)$.

4. Conclusion

In summary, we have measured a ballistic AB ring in two different probe configurations and found that some of the features like oscillation amplitude and magnetic field reversal symmetry are well explained within the LB framework. The analysis of the temperature dependence of the AB amplitude reveals that τ_ϕ depends on the probe configuration, and quantum decoherence is suppressed in the nonlocal meausurement. While the origin is not fully understood at this moment, its elucidation should shed new light on the mechanism of decoherence.

We thank H. Ebisawa and H. Fukuyama for helpful discussion. This work is partly supported by a Grant-in-Aid for Scientific Research and by a Grant-in-Aid for COE Research (“Quantum Dot and Its Application”) from the Ministry of Education, Culture, Sports, Science, and Technology.

References

[1] Büttiker M 1986 Phys. Rev. Lett. 57 1761
[2] Yacoby A, Sivan U, Umbach C P and Hong J M 1991 Phys. Rev. Lett. 66 1938
[3] Seelig G and Büttiker M 2001 Phys. Rev. B 64 245313
[4] Büttiker M 1988 IBM J. Res. Develop. 32 317